*Real-Time RT-PCR*

To quantify gene expression level, real-time RT-PCR was conducted using total RNA (1 μg) extracted from each cell line or tumor tissue, according to the manufacturer's instructions.[17] Primers and probes for each gene were designed using the Probe Finder software in the Universal Probe Library Assay Design Center (Roche). The expression level of each gene was normalized as a ratio to that of actin beta *(ACTB)* in vivo, and hypoxanthine phosphoribosyltransferase 1 *(HPRT1)* in in vitro experiments.

*Cadherin 13 Knockdown Experiment*

To downregulate endogenous cadherin 13 *(CDH13)* expression in U251, we used 2 Stealth small interfering RNAs (siRNAs) targeting *CDH13* that had been custom-synthesized by Invitrogen. Sequences of the 2 siRNAs are 1): sense primer 5′-TATTGTTGATCTTGGAGATCT TCCA-3′ and antisense primer 5′-TGGAAGATCTCCA AGATCAACAATA-3′; and 2): sense primer 5′-ATAAA CAGCGATTACTTCTCTGTCC-3′ and antisense primer 5′-GGACAGAGAAGTAATCGCTGTTTAT-3′.

Stealth siRNA negative control duplexes (Invitrogen) whose guanine-cytosine content was close to that of each duplex siRNA were used as controls. The U251 cells were seeded in 24-well plates at a density of $2 \times 10^4$ cells/well, and then transfected with the Stealth or control siRNA using Lipofectamine RNAiMAX transfection agent (Invitrogen) according to the manufacturer's recommended procedure.

*Western Blot Analysis*

Western blot analysis was performed to confirm *CDH13* levels using anti-*CDH13* polyclonal antibody (ab50846; Abcam). Whole cell lysates were extracted from U251 72 hours after transfection with Stealth or control siRNA, separated using 15% sodium dodecyl sulfate polyacrylamide gels, and transferred to a polyvinylidene difluoride membrane. The membranes were incubated with *CDH13* antibody or glyceraldehyde 3-phosphate dehydrogenase (*GAPDH*, ab8245; Abcam) as an internal control. Immunoreactive proteins were visualized using horseradish peroxidase–linked anti–rabbit (W401B; Promega) or anti–mouse immunoglobulin (NA931; GE Healthcare) using the ECL-Plus system (GE Healthcare) and luminoimage analyzer (LAS-4000 mini, FujiFilm Corp.).

*In Vitro PpIX Fluorescence Molecular Imaging*

After incubation in serum-free DMEM containing 5-ALA solution (final concentration 400 μM) for 6 hours at 37°C, PpIX-specific fluorescence in cells was captured by fluorescence microscopy (Olympus IX71 inverted microscope) and a digital camera (Olympus DP71) under the same exposure times. Intracellular PpIX was excited at a wavelength of 407 nm, and molecular images were collected in the red channel through 655-nm long-pass filters.

*In Vitro PpIX Fluorescence Intensity Analysis*

The A1207, NMCG1, U373, and U251 cells ($5 \times 10^5$ cells) were incubated with serum-free DMEM for 12 hours to adhere tightly to culture dishes and then exposed to 5-ALA (final concentration 400 μM) for 6 hours at 37°C. The cells were collected, resuspended in 100-μl extraction solution (50 mM Tris-HCl, pH 7.5; 100 mM NaCl; 2.5% Triton X-100), shaken for 1 minute at room temperature, and centrifuged at 15,000 rpm for 5 minutes. The supernatant was transferred into 300 μl of ethyl acetate and glacial acetic acid solution (V/V, 2:1). After 1 minute of vigorous shaking, 300 μl of 0.6 M NaOH was added to the supernatant and centrifuged at 15,000 rpm for 2 minutes. The upper phase was dissolved in 300 μl of 0.5 M HCl and centrifuged at 15,000 rpm for 2 minutes, and then the lower phase was collected and read for PpIX fluorescence using the ARVO MX plate reader (Perkin-Elmer).

In *CDH13* knockdown experiments, U251 cells were incubated with *CDH13* siRNA no. 1 to attenuate *CDH13* expression in 24-well plates at 37°C for 72 hours, and then the media in each well were replaced with serum-free DMEM containing 5-ALA solution. After the 6-hour incubation, PpIX was extracted and PpIX fluorescence intensity was measured using the protocol detailed above. In *CDH13* knockdown experiments, the fluorescence intensity of PpIX was normalized as a ratio to total protein content to correct variations in the number of cells in each well.

## Results

*Selection of Genes Related to 5-ALA–Induced Tumor Fluorescence Signal*

We used a total of 22 samples collected from 11 of the 16 patients as analytical grade tumors. Of these 11 patients, 4 were female and 7 were male; the median age was 45 years old (range 2–80 years old). The tumors included 7 glioblastomas, 1 anaplastic astrocytoma, 1 anaplastic ependymoma, 1 oligoastrocytoma, and 1 pilocytic astrocytoma, and all of the tumors were displayed as strongly enhanced rings and/or solid tumor masses with surrounding edema using preoperative Gd-enhanced MRI.

To screen genes overexpressed only in 5-ALA–induced fluorescence-negative tumors, we performed comprehensive gene expression analysis using microarrays in 11 pairs of tumor specimens showing and not showing 5-ALA–induced fluorescence. A total of 5606 probes were evaluated for their ability to analyze expression levels, and 2 statistical methods (a fold-change value analysis and the SAM method) provided 500 and 2000 possible probes as candidates, respectively. Among those that fulfilled both of these criteria, we chose 251 probes that showed remarkably high expression only in fluorescent-negative tumors (median intensity of expression signal > 1.0). We then selected 68 cancer-related genes (80 probes) as functionally annotated by the Ingenuity Pathways Analysis Knowledge Base, and finally pinpointed *CDH13*, known as a tumor suppressor gene,[31] as the most likely determinant of a 5-ALA–induced fluorescence signal in glioma. In general, a tumor suppressor gene is related to the malignancy of a tumor, which is believed to be corre-

lated with a positive rate of 5-ALA–induced fluorescence signal.[6,21,26,27]

The relevance of *CDH13* expression to 5-ALA–induced fluorescence in tumor tissues was confirmed in the quantified expression levels. Real-time RT-PCR analysis followed by a paired t-test revealed that the expression level of *CDH13* was significantly higher in fluorescence-negative tumors (mean 0.09388, range 0.00135–0.34966) than in corresponding fluorescence-positive tumor tissues (mean 0.04610, range 0.00004–0.25442; $p = 0.027$), although the *CDH13* expression levels varied significantly among tumors (Fig. 1). The increased expression in fluorescence-negative tumors was observed in 8 of 11 pairs of tumor samples, but not in 3 pairs of tumor specimens with extremely low *CDH13* expression.

### *Significance of Selected Gene as a Determinant of 5-ALA–Induced Fluorescence Signal*

Cadherin 13 might participate in the 5-ALA–induced fluorescence pathway. To evaluate its functional significance in the pathway, PpIX accumulation—the critical cause of bright fluorescence upon excitation with blue light—along with the *CDH13* expression was measured in 4 glioma cell lines (U373, U251, A1207, and NMCG1). The relative expression levels of *CDH13* in U251, A1207, and NMCG1 were 4.5-, 7.7-, and 17.1-fold, respectively, compared with U373 cells (Fig. 2). On the other hand, intensities of fluorescence by accumulated PpIX after exposure to 5-ALA were significantly lower in U251, A1207, and NMCG1 cells than in U373 cells ($p < 0.001$ for all 3, respectively, using the Dunnett test), although the fluorescence intensity in NMCG1 was not lower than that in A1207.

The results shown in NMCG1 encouraged us to perform *CDH13* knockdown experiments in U251 cells using specific siRNAs to elucidate the relevance of *CDH13* expression to 5-ALA–induced fluorescence. The knockdown experiments clearly demonstrated enhancement of 5-ALA–induced fluorescence associated with reduced expression of *CDH13*, both in the protein and mRNA levels (Fig. 3A–C). Furthermore, PpIX fluorescence intensity analysis revealed that *CDH13* knockdown caused an approximately 13-fold increase of PpIX accumulation (normalized by the amount of total protein) in U251 cells (Fig. 3D).

In general, knockdown of the tumor suppressor gene causes an increase in cell viability, which was confirmed also in *CDH13*: 3′(4,5-dimethylthiazol-2-yl)2,5-diphenyltetrazolium bromide assay after *CDH13* siRNA treatment demonstrated a significant increase in the number of viable cells in U251 after *CDH13* knockdown ($p < 0.001$).

### *Possible Role of CDH13 in PpIX Accumulation Pathway*

Cadherin 13 may play some important role in accumulation of PpIX and proliferation in tumor cells, thereby relating to 5-ALA–induced fluorescence. To clarify the role of *CDH13* in the PpIX accumulation pathway, we at-

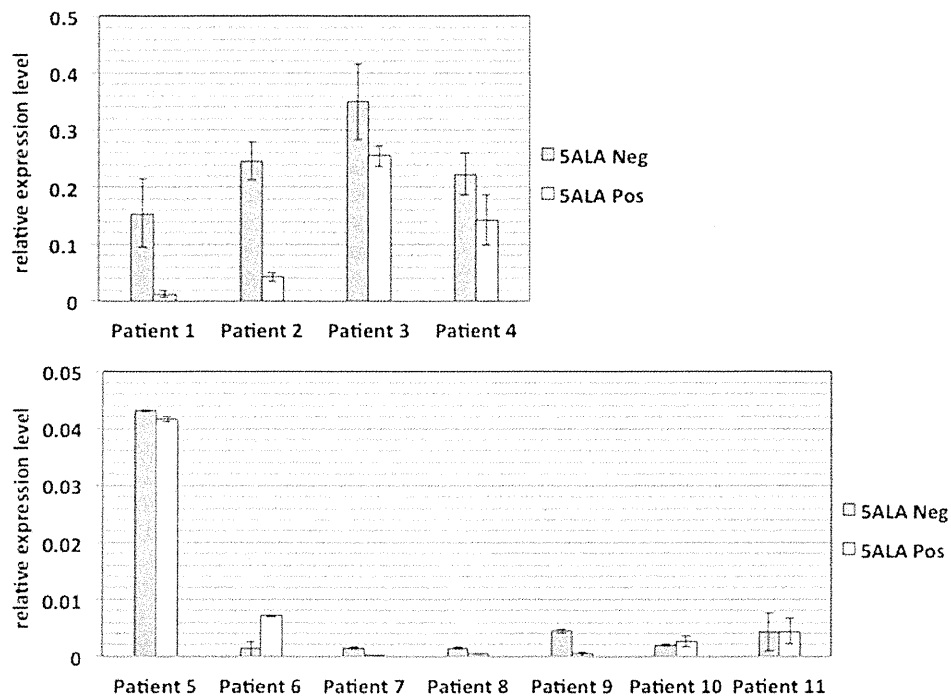


**Fig. 1.** Cadherin 13 expression levels and 5-ALA–induced fluorescence in glioma tissues. A total of 11 paired sets of tumor tissues, fluorescence-positive *(white bars)* and fluorescence-negative *(gray bars)* samples, were collected from 11 patients who had undergone 5-ALA–guided resection. The *CDH13* expression levels in tissue specimens were measured by real-time RT-PCR and normalized to *ACTB*. Because the expression levels varied significantly among tumors, 2 graphs were made **(upper and lower)** according to the relative expression level. Statistical differences in *CDH13* expression were analyzed using the paired t-test.

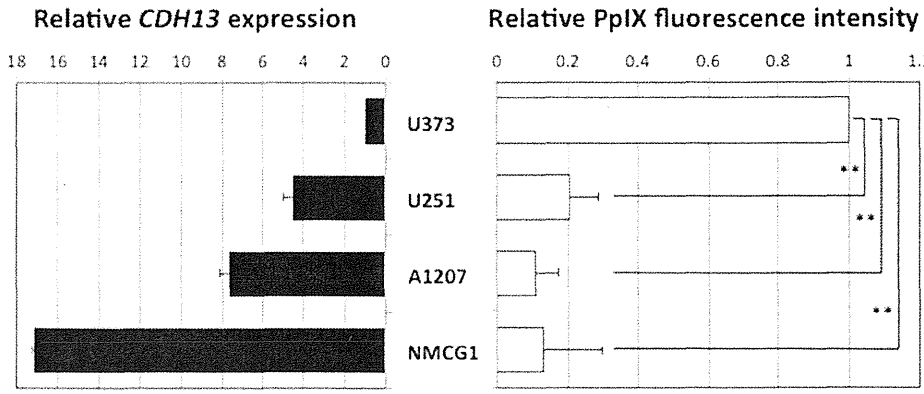


**Fig. 2.** Expression of *CDH13* and 5-ALA–induced PpIX accumulation in glioma cells. In 4 human glioma cell lines, *CDH13* expression **(left)** was analyzed using real-time RT-PCR and compared with 5-ALA–induced PpIX accumulation **(right)** measured using PpIX fluorescence intensity analysis. Both *CDH13* expression levels and PpIX fluorescence intensities were described as relative values to the mean value of those in U373. Data are expressed as mean ± SD, from 3 independent experiments. Multiple comparisons of PpIX fluorescence intensity were conducted using 1-way ANOVA, followed by the Dunnett test. ** $p < 0.001$.

tempted to find another important factor that was functionally related to *CDH13* in the PpIX accumulation pathway. Microarray analysis was performed on U251 cells treated with siRNA or control for 72 hours. Comparison of the gene expression data between cells transfected with control and *CDH13* siRNA no. 1 showed that 179 genes were significantly upregulated, while 237 were downregulated, in association with the *CDH13* knockdown. Among these, there were 2 possible genes that might be involved in the porphyrin biosynthesis: ATP-binding cassette transporter *ABCG2*, the pump for discharging PpIX out of cells, and *PEPT1*, which transports 5-ALA

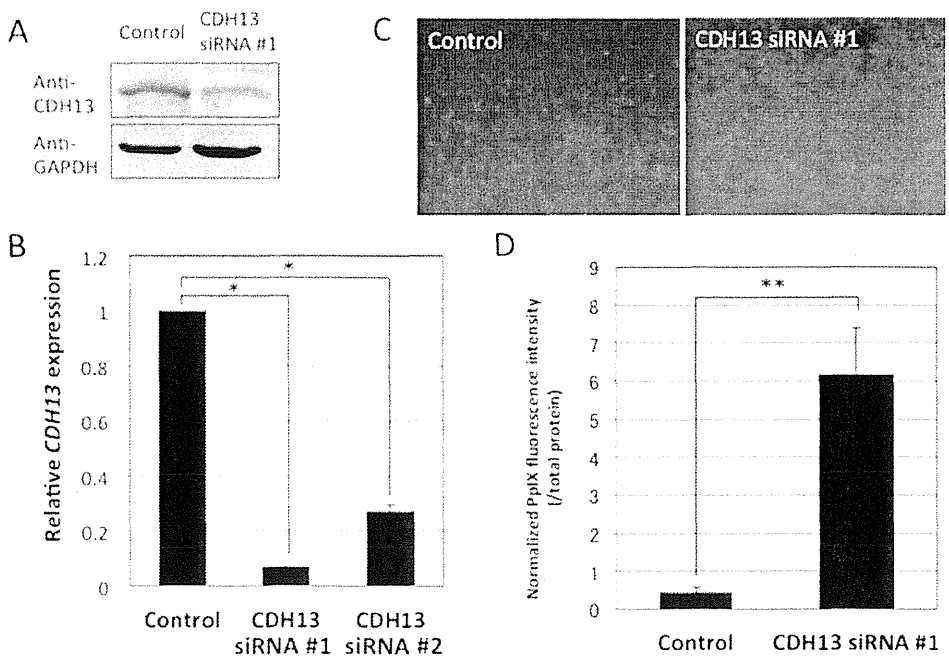


**Fig. 3.** Effect of *CDH13* knockdown on 5-ALA–induced PpIX accumulation and fluorescence in U251 cells. The *CDH13* knockdown experiments were performed in U251 cells to elucidate the relevance of *CDH13* expression to 5-ALA–induced fluorescence. The specific siRNAs (*CDH13* siRNA #1 and #2) successfully reduced CDH13 expression in both the protein **(A)** and mRNA levels **(B)**. The amount of CDH13 protein was measured at 72 hours after transfection of siRNA #1 into U251 cells. Glyceraldehyde 3-phosphate dehydrogenase is included as a loading control (A). The *CDH13* mRNA levels were measured by real-time RT-PCR 24 hours after transfection in U251 cells and are shown as relative value to the mean value of the control. Data are expressed as mean ± SD, from 3 independent experiments (B). Cadherin 13 knockdown increased 5-ALA–induced fluorescence in U251 cells treated with 5-ALA at a concentration of 400 μM for 6 hours, which was observed in both PpIX fluorescence molecular imaging **(C)** and PpIX fluorescence intensity analysis **(D)**. The 5-ALA–induced PpIX accumulation in *CDH13* knockdown cells was measured by PpIX fluorescence intensity analysis in 24-well plates, and the fluorescence intensity of PpIX was normalized to total protein content to correct any variation in the number of cells in each well. Data are presented as mean ± SD from 4 independent experiments (D). Statistical analysis was performed using the t-test. * $p < 0.05$, ** $p < 0.001$.

into the cells. The *ABCG2* expression levels in *CDH13* knockdown cells were 7.3% of the control with microarray analysis (Table 1), which was confirmed in the quantified expression levels measured by real-time RT-PCR ($p < 0.001$; Fig. 4). On the other hand, *CDH13* knockdown caused a 12.5-fold increase of *PEPT1* expression compared with the control (Table 1).

There are 10 other possible factors that have already been shown to be involved in porphyrin biosynthesis: ABC transporter *ABCB6*, aminolevulinate dehydratase *(ALAD)*, aminolevulinate synthase 1, 2 *(ALAS1, ALAS2)*, coproporphyrinogen oxidase *(CPOX)*, *FECH*, hydroxymethylbilane synthase *(HMBS)*, protoporphyrinogen oxidase *(PPOX)*, uroporphyrinogen decarboxylase *(UROD)*, and uroporphyrinogen III synthase *(UROS)*.[12] However, *CDH13* knockdown did not cause any significant alteration in expression levels of these factors (Table 1).

## Discussion

In this study, *CDH13* was suggested to play some important roles in the PpIX accumulation pathway, indicating that it is a key regulator of 5-ALA–induced fluorescence in glioma cells. Despite several discrepant results, *CDH13* was shown to be overexpressed, mostly in 5-ALA–induced fluorescence-negative tumors, and related to the pathway of PpIX accumulation. The downregulation of *CDH13* expression facilitated PpIX accumulation through the regulation of important factors such as *PEPT1* and *ABCG2* in the PpIX accumulation pathway in glioma cells. Cadherin 13 thus could be a potent candidate molecule in the new approach to enhance 5-ALA–induced fluorescence in brain tumors, which might lead to improvement in 5-ALA–guided resection, and thus curative resection rates for gliomas.

Cadherin 13 is a member of the cadherin superfamily and is highly expressed in the nervous system.[31] A variety of studies have demonstrated the functional role of *CDH13* in cell proliferation, the cell cycle, and epigenetic silencing in cancer, and *CDH13* is now recognized as a tumor suppressor gene. *CDH13* is believed to suppress the development of neural cells[31] and induce G2 (premiotic phase) arrest in astrocytomas via p21.[8] The expression of *CDH13* is downregulated through methylation in breast, ovarian, and lung cancer,[2] is suggested as an early marker for lung cancer,[6] and is a potent predictor of poor prognosis in lung, ovarian, and esophageal cancers.[2] Despite numerous studies on tumor suppressor genes, this study may be the first to show the possible role of *CDH13* in PpIX biosynthesis pathways.

Protoporphyrin IX biosynthesis pathways have been intensively investigated for PpIX accumulation induced by 5-ALA, but the details remain unknown. Numerous studies have been conducted to elucidate the mechanisms and critical factors in the pathway. Recent studies demonstrated that *FECH* and *CPOX* might be included in PpIX biosynthesis pathways and accumulation of PpIX in gliomas;[30,32] more recently, downregulation of *ABCG2* was suggested as a cause of increased PpIX accumulation in colorectal and cervical cancers.[5] The mechanisms, however, are now recognized to be multifactorial, and so none of the factors have been established as the principal one in the pathway. With the exception of *ABCB2*, this study did not demonstrate any significant roles for *FECH* and *CPOX*, as well as other suggested factors such as *ABCB6*, *ALAD*, *ALAS1*, *ALAS2*, *HMBS*, *PPOX*, *UROD*, and *UROS* in porphyrin biosynthesis.[12]

Our study may be the first attempt to perform a nonhypothetical screening of novel and important regulators of 5-ALA–induced PpIX accumulation using comprehensive gene expression analysis. To reduce the selection bias—individual variability of the gene expression profiles caused by age, sex, and others—we selected 22 tumor samples from 11 patients for pair-wise comparison of gene expression between positive and negative signal samples. Then we employed 2 different statistical selection methods for candidate genes—fold-change and SAM statistical values—and found 68 genes selectively overexpressed in negative signal samples as final candidates for clinical application in the future. Among these,

**TABLE 1: Influence of *CDH13* knockdown on gene expression related to PpIX biosynthesis pathways**

| Gene Symbol | Gene Name | Change of Gene Expression Caused by *CDH13* Knockdown | Expression Signal | |
|---|---|---|---|---|
| | | | *CDH13* Knockdown Cells | Negative Control Cells |
| *ABCB6* | *ATP-binding cassette, sub-family B (MDR/TAP), member 6* | −0.292 | 1.65 | 1.94 |
| *ABCG2* | *ATP-binding cassette, sub-family G (WHITE), member 2* | −3.777 | −4.38 | −0.6 |
| *ALAD* | *aminolevulinate, dehydratase* | 0.22 | −1.49 | −1.71 |
| *ALAS1* | *aminolevulinate, delta-, synthase 1* | −0.482 | 0.43 | 0.91 |
| *ALAS2* | *aminolevulinate, delta-, synthase 2* | 0.02 | −7.73 | −7.75 |
| *CPOX* | *coproporphyrinogen oxidase* | −0.218 | −0.18 | 0.04 |
| *FECH* | *ferrochelatase* | 0.06 | −0.12 | −0.18 |
| *HMBS* | *hydroxymethylbilane synthase* | −1.135 | 2.96 | 4.1 |
| *PEPT1* | *oligopeptide transporter 1* | 3.64 | −3.52 | −7.17 |
| *PPOX* | *protoporphyrinogen oxidase* | 0.097 | 1.41 | 1.31 |
| *UROD* | *uroporphyrinogen decarboxylase* | 0.095 | 4.9 | 4.8 |
| *UROS* | *uroporphyrinogen III synthase* | −0.87 | −1.17 | −0.3 |

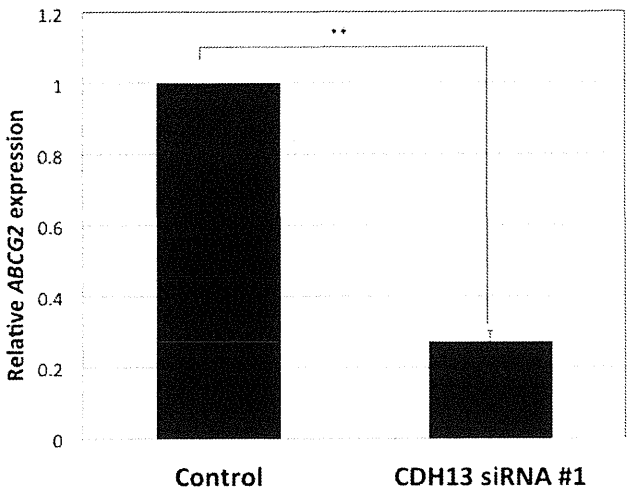


FIG. 4. Effects of *CDH13* knockdown on *ABCG2* expression in U251. The *ABCG2* mRNA levels were measured by real-time RT-PCR at 72 hours after transfection with *CDH13* siRNA #1. Expression of *ABCG2* is shown as relative value to the mean value in the control. Data are expressed as mean ± SD, from 3 independent experiments. Statistical analysis was performed using the t-test. ** $p < 0.001$.

we selected genes that were believed to be related to tumor progression because positive response to 5-ALA in fluorescence induction is suggested as being closely correlated with malignant grade of glioma.[6,21,26,27] The final candidate genes included only 1 tumor suppressor gene, *CDH13*, and the functional significance of *CDH13* as a negative regulator of 5-ALA–induced fluorescence was shown in in vitro experiments, so we believe that this selection approach can elucidate more detailed PpIX biosynthesis pathways.

We measured the amount of PpIX using fluorescence intensity analysis instead of direct PpIX measurement, thinking the former might have advantages in fluorescence quantification over other detection methods[10,16,23] Our results of the association between *CDH13* expression and amount of intracellular PpIX in cell lines and tumor specimens strongly suggested that the *CDH13* might act on PpIX accumulation. Results clearly demonstrated that *CDH13* siRNA caused an increase of PpIX accumulation and 5-ALA–induced fluorescence in glioma cells, suggesting that *CDH13* downregulation can improve the accuracy of PpIX fluorescence-guided discrimination of malignant cells. Even so, the mechanism or mechanisms of fluorescence augmentation by *CDH13* knockdown remains undetermined. Observed correlations of *CDH13* with PpIX accumulation and 5-ALA–induced fluorescence in tumor tissues were less robust as compared with those in tumor cells. This might be due to the technical issues of the existing detection methods, at least in part, but also suggests the existence of a more complicated mechanism underlying the variable response to 5-ALA in tumor.

We also found that *ABCG2* and *PEPT1* showed altered expression levels associated with a modification of *CDH13* expression. *ABCG2* is well known as an ATP-binding efflux pump of porphyrin, indicating that the pump may be involved in the fluorescence induction mechanism of 5-ALA through the regulation of porphyrin transport.[1,35] In fact, inhibition of the *ABCG2* transporter has been shown to improve the efficacy of photodynamic therapy in keratinocytes.[3] Thus, our hypothesis is that *CDH13* downregulation may act on *ABCG2* to reduce the expression level and inhibit the efflux of PpIX and increase the accumulation of PpIX in glioma. We also revealed that *PEPT1* was upregulated in response to the *CDH13* downregulation in U251 cells. *PEPT1* is a 5-ALA influx transporter that may enhance PpIX accumulation,[19] although the expression level of *PEPT1* in control cells was extremely low and thus the increased effect was not definitive in this study. Some reports have found that *CDH13* possibly interacts with a transmembrane receptor, such as receptor tyrosine kinases or G protein-coupled receptors, to send a signal to Akt.[2] Given all of these data, *CDH13* might determine the intensity of the tumor fluorescence signal induced by 5-ALA by regulating PpIX accumulation into cells with modification of *ABCG2* and *PEPT1* expression via these signaling cascades. At present, the precise mechanisms remain unclear. We continue to intensely study the interaction of *CDH13* on *ABCB2* and *PEPT1* and the mechanistic roles in PpIX accumulation, along with a validation study of the correlation between CDH13 expression level and 5-ALA–induced fluorescence using more tumor specimens that showed different levels of fluorescence.

## Conclusions

Our study demonstrated that *CDH13* might be the noteworthy factor in the mechanism of the 5-ALA–induced fluorescence signal, and its knockdown could enhance the intensity of the 5-ALA–induced fluorescence signal through an increase of PpIX accumulation in glioma cells. These new findings might lead a novel fluorescent indicator to overcome the obstacles of existing fluorescence-guided resection and improve the limited resection rate. Nevertheless, the details of *CDH13* actions in the 5-ALA metabolic pathway, including the interaction with *ABCB2* and *PEPT1*, remain unknown. Other than our suggested factors, there are several possible factors that might be involved in porphyrin biosynthesis, such as *FECH* and *CPOX*, but their functional significances remain controversial.[12] Further studies to clarify the roles of *CDH13* in the 5-ALA metabolic pathway are strongly required, along with studies involving the clinical application of these findings.

### Acknowledgments

We thank Mss. Hitomi Miyabara, Azusa Sekine, Chieko Yanagidate, Chika Kumazawa, and Kyoko Totake for their enormous efforts and skillful technical assistance.

### Disclosure

This study was performed as a research program of the Project for Development of Innovative Research on Cancer Therapeutics (P-Direct) from the Ministry of Education, Culture, Sport, Science, and Technology, Japan (MEXT). Additional support was provided by the National Cancer Center Research and Development Fund

(grant no. 23-A-20), the Strategic Research Foundation Grant-aided Project for Private Universities, MEXT (grant no. S0801004), and a Saitama Medical University Internal Grant (no. 08-1-1-11).

Author contributions to the study and manuscript preparation include the following. Conception and design: Nishiyama, Suzuki, Wada, Matsutani, Nishikawa. Acquisition of data: Suzuki, Wada, Eguchi, Adachi, Mishima, Nishikawa. Analysis and interpretation of data: Nishiyama, Suzuki, Wada, Eguchi, Adachi. Drafting the article: Nishiyama, Suzuki, Wada. Critically revising the article: all authors. Reviewed submitted version of manuscript: all authors. Approved the final version of the manuscript on behalf of all authors: Nishiyama. Statistical analysis: Wada, Eguchi. Administrative/technical/material support: Mishima, Matsutani, Nishikawa. Study supervision: Nishiyama, Nishikawa.

## References


1. An R, Hagiya Y, Tamura A, Li S, Saito H, Tokushima D, et al: Cellular phototoxicity evoked through the inhibition of human ABC transporter ABCG2 by cyclin-dependent kinase inhibitors in vitro. **Pharm Res 26:**449–458, 2009
2. Andreeva AV, Kutuzov MA: Cadherin 13 in cancer. **Genes Chromosomes Cancer 49:**775–790, 2010
3. Bebes A, Nagy T, Bata-Csörgo Z, Kemény L, Dobozy A, Széll M: Specific inhibition of the ABCG2 transporter could improve the efficacy of photodynamic therapy. **J Photochem Photobiol B 105:**162–166, 2011
4. Bisland SK, Goebel EA, Hassanali NS, Johnson C, Wilson BC: Increased expression of mitochondrial benzodiazepine receptors following low-level light treatment facilitates enhanced protoporphyrin IX production in glioma-derived cells in vitro. **Lasers Surg Med 39:**678–684, 2007
5. Gupta N, Martin PM, Miyauchi S, Ananth S, Herdman AV, Martindale RG, et al: Down-regulation of BCRP/ABCG2 in colorectal and cervical cancer. **Biochem Biophys Res Commun 343:**571–577, 2006
6. Hefti M, von Campe G, Moschopulos M, Siegner A, Looser H, Landolt H: 5-aminolevulinic acid induced protoporphyrin IX fluorescence in high-grade glioma surgery: a one-year experience at a single institutuion. **Swiss Med Wkly 138:**180–185, 2008
7. Hinnen P, de Rooij FW, van Velthuysen ML, Edixhoven A, van Hillegersberg R, Tilanus HW, et al: Biochemical basis of 5-aminolaevulinic acid-induced protoporphyrin IX accumulation: a study in patients with (pre)malignant lesions of the oesophagus. **Br J Cancer 78:**679–682, 1998
8. Huang ZY, Wu Y, Hedrick N, Gutmann DH: T-cadherin-mediated cell growth regulation involves G2 phase arrest and requires p21(CIP1/WAF1) expression. **Mol Cell Biol 23:**566–578, 2003
9. Iacob G, Dinca EB: Current data and strategy in glioblastoma multiforme. **J Med Life 2:**386–393, 2009
10. Inoue H, Kajimoto Y, Shibata MA, Miyoshi N, Ogawa N, Miyatake S, et al: Massive apoptotic cell death of human glioma cells via a mitochondrial pathway following 5-aminolevulinic acid-mediated photodynamic therapy. **J Neurooncol 83:**223–231, 2007
11. Ishikawa T, Nakagawa H, Hagiya Y, Nonoguchi N, Miyatake S, Kuroiwa T: Key role of human ABC transporter ABCG2 in photodynamic therapy and photodynamic diagnosis. **Adv Pharmacol Sci 2010:**587306, 2010
12. Krishnamurthy P, Xie T, Schuetz JD: The role of transporters in cellular heme and porphyrin homeostasis. **Pharmacol Ther 114:**345–358, 2007
13. Lacroix M, Abi-Said D, Fourney DR, Gokaslan ZL, Shi W, DeMonte F, et al: A multivariate analysis of 416 patients with glioblastoma multiforme: prognosis, extent of resection, and survival. **J Neurosurg 95:**190–198, 2001
14. Lefranc F, Sadeghi N, Camby I, Metens T, Dewitte O, Kiss R: Present and potential future issues in glioblastoma treatment. **Expert Rev Anticancer Ther 6:**719–732, 2006
15. Li F, Glinskii OV, Zhou J, Wilson LS, Barnes S, Anthony DC, et al: Identification and analysis of signaling networks potentially involved in breast carcinoma metastasis to the brain. **PLoS ONE 6:**e21977, 2011
16. Miyake M, Ishii M, Kawashima K, Kodama T, Sugano K, Fujimoto K, et al: siRNA-mediated knockdown of the heme synthesis and degradation pathways: modulation of treatment effect of 5-aminolevulinic acid-based photodynamic therapy in urothelial cancer cell lines. **Photochem Photobiol 85:**1020–1027, 2009
17. Mohammed Ael S, Eguchi H, Wada S, Koyama N, Shimizu M, Otani K, et al: TMEM158 and FBLP1 as novel marker genes of cisplatin sensitivity in non-small cell lung cancer cells. **Exp Lung Res 38:**463–474, 2012
18. Nabavi A, Thurm H, Zountsas B, Pietsch T, Lanfermann H, Pichlmeier U, et al: Five-aminolevulinic acid for fluorescence-guided resection of recurrent malignant gliomas: a phase II study. **Neurosurgery 65:**1070–1077, 2009
19. Neumann J, Brandsch M: Delta-aminolevulinic acid transport in cancer cells of the human extrahepatic biliary duct. **J Pharmacol Exp Ther 305:**219–224, 2003
20. Ruge JR, Liu J: Use of 5-aminolevulinic acid for visualization and resection of a benign pediatric brain tumor. Case report. **J Neurosurg Pediatr 4:**484–486, 2009
21. Sanai N, Snyder LA, Honea NJ, Coons SW, Eschbacher JM, Smith KA, et al: Intraoperative confocal microscopy in the visualization of 5-aminolevulinic acid fluorescence in low-grade gliomas. Clinical article. **J Neurosurg 115:**740–748, 2011
22. Sano H, Wada S, Eguchi H, Osaki A, Saeki T, Nishiyama M: Quantitative prediction of tumor response to neoadjuvant chemotherapy in breast cancer: novel marker genes and prediction model using the expression levels. **Breast Cancer 19:**37–45, 2012
23. Sinha AK, Anand S, Ortel BJ, Chang Y, Mai Z, Hasan T, et al: Methotrexate used in combination with aminolaevulinic acid for photodynamic killing of prostate cancer cells. **Br J Cancer 95:**485–495, 2006
24. Smith JS, Chang EF, Lamborn KR, Chang SM, Prados MD, Cha S, et al: Role of extent of resection in the long-term outcome of low-grade hemispheric gliomas. **J Clin Oncol 26:** 1338–1345, 2008
25. Stepp H, Beck T, Pongratz T, Meinel T, Kreth FW, Tonn JCh, et al: ALA and malignant glioma: fluorescence-guided resection and photodynamic treatment. **J Environ Pathol Toxicol Oncol 26:**157–164, 2007
26. Stummer W, Novotny A, Stepp H, Goetz C, Bise K, Reulen HJ: Fluorescence-guided resection of glioblastoma multiforme by using 5-aminolevulinic acid-induced porphyrins: a prospective study in 52 consecutive patients. **J Neurosurg 93:** 1003–1013, 2000
27. Stummer W, Pichlmeier U, Meinel T, Wiestler OD, Zanella F, Reulen HJ: Fluorescence-guided surgery with 5-aminolevulinic acid for resection of malignant glioma: a randomised controlled multicentre phase III trial. **Lancet Oncol 7:**392–401, 2006
28. Stummer W, Stocker S, Wagner S, Stepp H, Fritsch C, Goetz C, et al: Intraoperative detection of malignant gliomas by 5-aminolevulinic acid-induced porphyrin fluorescence. **Neurosurgery 42:**518–526, 1998
29. Stupp R, Mason WP, van den Bent MJ, Weller M, Fisher B, Taphoorn MJ, et al: Radiotherapy plus concomitant and adjuvant temozolomide for glioblastoma. **N Engl J Med 352:**987–996, 2005
30. Takahashi K, Ikeda N, Nonoguchi N, Kajimoto Y, Miyatake S, Hagiya Y, et al: Enhanced expression of coproporphyrinogen oxidase in malignant brain tumors: CPOX expression and

5-ALA-induced fluorescence. **Neuro Oncol 13:**1234–1243, 2011
31. Takeuchi T, Misaki A, Liang SB, Tachibana A, Hayashi N, Sonobe H, et al: Expression of T-cadherin (CDH13, H-Cadherin) in human brain and its characteristics as a negative growth regulator of epidermal growth factor in neuroblastoma cells. **J Neurochem 74:**1489–1497, 2000
32. Teng L, Nakada M, Zhao SG, Endo Y, Furuyama N, Nambu E, et al: Silencing of ferrochelatase enhances 5-aminolevulinic acid-based fluorescence and photodynamic therapy efficacy. **Br J Cancer 104:**798–807, 2011
33. Tonn JC, Stummer W: Fluorescence-guided resection of malignant gliomas using 5-aminolevulinic acid: practical use, risks, and pitfalls. **Clin Neurosurg 55:**20–26, 2008
34. Tusher VG, Tibshirani R, Chu G: Significance analysis of microarrays applied to the ionizing radiation response. **Proc Natl Acad Sci U S A 98:**5116–5121, 2001
35. Wakabayashi K, Tamura A, Saito H, Onishi Y, Ishikawa T: Human ABC transporter ABCG2 in xenobiotic protection and redox biology. **Drug Metab Rev 38:**371–391, 2006

Manuscript submitted December 11, 2012.
Accepted July 22, 2013.
Please include this information when citing this paper: published online September 6, 2013; DOI: 10.3171/2013.7.JNS122340.
*Address correspondence to:* Masahiko Nishiyama, M.D., Ph.D., Department of Molecular Pharmacology and Oncology, Gunma University Graduate School of Medicine, 3-39-22 Showa-machi, Maebashi, Gunma 371-8511, Japan. email: m.nishiyama@gunma-u.ac.jp.

J Neurosurg 119:845–852, 2013


# Phase II clinical study on intraoperative photodynamic therapy with talaporfin sodium and semiconductor laser in patients with malignant brain tumors

## Clinical article

YOSHIHIRO MURAGAKI, M.D., PH.D.,[1,2] JIRO AKIMOTO, M.D., D.MED.SCI.,[3] TAKASHI MARUYAMA, M.D., PH.D.,[1,2] HIROSHI ISEKI, M.D., PH.D.,[1,2] SOKO IKUTA, PH.D.,[1] MASAYUKI NITTA, M.D., PH.D.,[1,2] KATSUYA MAEBAYASHI, M.D., PH.D.,[4] TAIICHI SAITO, M.D., PH.D.,[1,5] YOSHIKAZU OKADA, M.D., PH.D.,[2] SADAO KANEKO, M.D.,[6] AKIRA MATSUMURA, M.D., PH.D.,[7] TOSHIHIKO KUROIWA, M.D., PH.D.,[8] KATSUYUKI KARASAWA, M.D., PH.D.,[9] YOICHI NAKAZATO, M.D., PH.D.,[10] AND TAKAMASA KAYAMA, M.D., PH.D.[11]

*[1]Faculty of Advanced Techno-Surgery, Institute of Advanced Biomedical Engineering and Science, and Departments of [2]Neurosurgery and [4]Radiation Oncology, Tokyo Women's Medical University, Tokyo; [3]Department of Neurosurgery, Tokyo Medical University, Tokyo; [5]Department of Neurosurgery, Hiroshima University, Hiroshima; [6]Kashiwaba Neurosurgical Hospital, Sapporo; [7]Department of Neurosurgery, University of Tsukuba, Ibaragi; [8]Department of Neurosurgery, Osaka Medical College, Osaka; [9]Department of Radiology, Tokyo Metropolitan Cancer and Infectious Diseases Center, Komagome Hospital, Tokyo; [10]Department of Human Pathology, Gunma University Graduate School of Medicine, Gunma; and [11]Department of Neurosurgery, Yamagata University, Yamagata, Japan*

*Object.* The objective of the present study was to perform a prospective evaluation of the potential efficacy and safety of intraoperative photodynamic therapy (PDT) using talaporfin sodium and irradiation using a 664-nm semiconductor laser in patients with primary malignant parenchymal brain tumors.

*Methods.* In 27 patients with suspected newly diagnosed or recurrent primary malignant parenchymal brain tumors, a single intravenous injection of talaporfin sodium (40 mg/m$^2$) was administered 1 day before resection of the neoplasm. The next day after completion of the tumor removal, the residual lesion and/or resection cavity were irradiated using a 664-nm semiconductor laser with a radiation power density of 150 mW/cm$^2$ and a radiation energy density of 27 J/cm$^2$. The procedure was performed 22–27 hours after drug administration. The study cohort included 22 patients with a histopathologically confirmed diagnosis of primary malignant parenchymal brain tumor. Thirteen of these neoplasms (59.1%) were newly diagnosed glioblastomas multiforme (GBM).

*Results.* Among all 22 patients included in the study cohort, the 12-month overall survival (OS), 6-month progression-free survival (PFS), and 6-month local PFS rates after surgery and PDT were 95.5%, 91%, and 91%, respectively. Among patients with newly diagnosed GBMs, all these parameters were 100%. Side effects on the skin, which could be attributable to the administration of talaporfin sodium, were noted in 7.4% of patients and included rash (2 cases), blister (1 case), and erythema (1 case). Skin photosensitivity test results were relatively mild and fully disappeared within 15 days after administration of photosensitizer in all patients.

*Conclusions.* Intraoperative PDT using talaporfin sodium and a semiconductor laser may be considered as a potentially effective and sufficiently safe option for adjuvant management of primary malignant parenchymal brain tumors. The inclusion of intraoperative PDT in a combined treatment strategy may have a positive impact on OS and local tumor control, particularly in patients with newly diagnosed GBMs. Clinical trial registration no.: JMA-IIA00026 (https://dbcentre3.jmacct.med.or.jp/jmactr/App/JMACTRS06/JMACTRS06.aspx?seqno=862).
*(http://thejns.org/doi/abs/10.3171/2013.7.JNS13415)*

**KEY WORDS • malignant brain tumor • malignant glioma • oncology • photodynamic therapy • talaporfin sodium • outcome**

MALIGNANT brain tumors are characterized by invasive growth into adjacent normal neuronal tissue. Therefore, it is crucial that their man-

This article contains some figures that are displayed in color online but in black-and-white in the print edition.

*Abbreviations used in this paper:* GBM = glioblastoma multiforme; OS = overall survival; PDT = photodynamic therapy; PFS = progression-free survival; PS = performance status; 5-ALA = 5-aminolevulinic acid.

agement is directed not only to maximal possible resection (while ensuring preservation of the functionally important anatomical structures), but on suppressing the growth of the residual infiltrative tumor cells. Despite aggressive surgical removal followed by postoperative radiotherapy and chemotherapy, between 50% and 85% of WHO Grade IV gliomas recur locally.[9,16] This emphasizes the need for additional options to improve their growth control.

Photodynamic therapy (PDT) is a treatment method that involves administration of a photosensitizer that accumulates in tumor tissue and newly formed neoplastic vessels. During subsequent irradiation with a laser beam of a specific wavelength, the photosensitizer undergoes a photochemical reaction that produces singlet oxygen possessing strong oxidation properties that cause alteration of the cells. Because singlet oxygen has a short lifetime (0.04–4 μsec), the PDT-induced cell death is realized only locally in the areas irradiated by the laser beam.[2,7,8,15]

Talaporfin sodium (mono-L-aspartyl chlorine e6, or NPe6) is a relatively novel photosensitizer for PDT. Its administration in combination with a semiconductor laser has been approved in Japan for clinical use in cases of early stage lung cancer. Nonclinical pharmacological studies directed to its possible application for management of malignant brain tumors were initiated starting in 2001.[12–14] Experiments with glioblastoma cell lines demonstrated that such therapy induces mitochondrial apoptotic cell loss accompanied by tumor necrosis.[13,14] Our recent single-center pilot clinical study on the use of talaporfin sodium and a semiconductor laser in patients with malignant gliomas demonstrated promising results with regard to tumor response rates and treatment safety.[1] Therefore, the present open-label, prospective, multicenter clinical trial was initiated for evaluation of the potential efficacy and safety of such therapy. This study was the first investigator-initiated clinical trial in Japan that planned to assess the use of talaporfin sodium and a semiconductor laser for intraoperative PDT as part of a combined management of primary malignant parenchymal brain tumors.

## Methods

Patients with suspected primary malignant parenchymal brain tumors, either newly diagnosed or recurrent, which according to preoperative neuroimaging corresponded to a WHO histopathological grade of III or IV,[11] were enrolled in this study. The recruitment of patients and analysis of treatment efficacy were mainly focused on newly diagnosed glioblastoma multiforme (GBM). The main inclusion criteria included agreement of the patient to provide written informed consent to participate in the study; age between 20 and 69 years at the time of informed consent; performance status (PS) score of 0, 1, 2, or 3 according to Eastern Cooperative Oncology Group PS scale (a PS score of 3 was accepted only when the score was attributable to neurological symptoms caused by the tumor); supratentorial location of the tumor not including neoplasms originating from the optic pathways and pituitary gland; absence of subarachnoid dissemination; and eligibility for aggressive resection of the lesion. The main exclusion criterion was a history of photosensitivity or porphyria.

### *Study Design*

This prospective clinical trial was developed and carried out in 2 neurosurgical centers with well-established neurooncology programs, namely Tokyo Women's Medical University and Tokyo Medical University. An open-label, investigator-initiated clinical study was conducted in accordance with the Declaration of Helsinki. The research protocol was approved by the Pharmaceuticals and Medical Devices Agency of Japan as well as by the ethics committees and institutional review boards of both participating universities. A special review board was formed for central radiology assessment, evaluation of data related to treatment efficacy and safety, and handling of the enrolled cases and overall data management. Additionally, a pathology board was created for central review of the permanent formalin-fixed tissue specimens to determine the histopathological tumor type and grade. The 3-year study period was scheduled from March 21, 2009, to February 28, 2012. The clinical trial information for this study can be found at https://dbcentre3.jmacct.med.or.jp/jmactr/App/JMACTRS06/JMACTRS06.aspx?seqno=862.

Patients who were considered eligible for enrollment into study received a single intravenous injection of talaporfin sodium (Laserphyrin, Meiji Seika Pharma Co., Ltd.) in a dose of 40 mg/m$^2$ on an inpatient basis 1 day prior to undergoing the elective craniotomy. The next day, surgery was done, the neoplasm was resected, and irradiation of the resection cavity with a 664-nm semiconductor laser beam (Panasonic Healthcare Co., Ltd.), with a diameter of 1.5 cm, radiation power density of 150 mW/cm$^2$, and radiation energy density of 27 J/cm$^2$, was performed. Particular emphasis was put on irradiation of the areas at risk for recurrence, such as the genu of the corpus callosum.[9] If tumor resection was incomplete and the residual lesion was macroscopically identified, additional irradiation by the laser was applied at 1 to 3 sites with avoidance of overlap of the irradiation areas. In all cases laser irradiation was done 22–27 hours after administration of talaporfin sodium.

### *Postoperative Treatment and Follow-Up*

Postoperatively all patients with newly diagnosed gliomas underwent fractionated radiotherapy (total dose 60 Gy) with concomitant and adjuvant chemotherapy using ACNU (in cases of WHO Grade III tumors) or temozolomide[18] (in cases of GBM). Patients with recurrent neoplasms were treated according to the preference of their doctors, taking into consideration the details of the primary management.

Adverse effects of treatment were graded according to the Common Terminology Criteria for Adverse Events version 3.0.[3] Follow-up examinations were performed every 2–3 months and included physical and neurological assessments with evaluation of PS score, blood and urine tests, and contrast-enhanced MRI. Tumor progression was defined as a 25% or greater increase in the volume of the contrast-enhanced lesion or the appearance of

new brain lesions. At the time of recurrence the salvage treatment was applied according to the preference of the individual doctors and usually included a combination of re-resection, second-line chemotherapy, and/or vaccine therapy.

*End Point Evaluation*

The primary end point of the study was overall survival (OS) rate at 12 months after PDT. Secondary end points were progression-free survival (PFS) and local PFS rates at 6 months after PDT. The OS, PFS, and local PFS were all estimated from the date of surgery. Additionally, in cases with a maximal diameter of the residual neoplasm of 16 mm or more, the overall tumor response to treatment was evaluated. All brain MRI data before surgery and during follow-up were assessed by review board members. Safety end points included rates of adverse events, side effects, and results of skin photosensitivity testing.

*Data Analysis*

Analysis of the treatment efficacy was done in all patients who underwent PDT based on administration of talaporfin sodium and intraoperative laser irradiation of the residual neoplasm and/or resection cavity if the diagnosis of primary malignant parenchymal brain tumor was confirmed by the pathology review board after investigation of the permanent formalin-fixed tissue sections (study cohort). Separate analysis of the treatment efficacy was also done in the subgroup of patients with newly diagnosed GBMs. Survival was assessed using the Kaplan-Meier method. Analysis of the treatment safety was done in all patients initially enrolled into the study who received talaporfin sodium.

## Results

*Patient Characteristics*

Detailed characteristics of patients enrolled in the study are presented in Table 1. In all, 27 patients initially received talaporfin sodium. However, 3 patients were deemed ineligible for study participation during surgery and did not receive irradiation with the laser based on the results of the intraoperative histopathological investigation of the resected tissue on the frozen sections, which revealed lymphoma, low-grade glioma, and cavernoma (1 case each). Additionally, 2 patients were excluded from the study later on because the pathology review board did not confirm the diagnosis of a primary malignant parenchymal brain tumor based on the postoperative examination of the permanent formalin-fixed tissue sections. Therefore, the study cohort included 22 patients with a male/female ratio of 1:1 and a median age of 50.5 years (range 24–69 years). The frontal lobe was affected most frequently (59.1% of cases). In 72.7% of patients the tumor was located within or close to eloquent brain areas. Total, subtotal (> 90% of the lesion volume), and partial resections of the neoplasm were performed in 36.4%, 50%, and 13.6% of cases, respectively. No significant differences in clinical characteristics were observed between the entire group of initially enrolled patients (n = 27) and the study cohort (n = 22). Thirteen (59.1%) of 22 patients included in the study cohort had newly diagnosed GBMs and corresponded to recursive partitioning analysis Classes III (4 cases), IV (5 cases), and V (4 cases).[6]

*Treatment Efficacy*

Among all 22 patients included in the study cohort, 1 death occurred within 12 months after surgery. This patient died 3.4 months after resection and PDT of a newly diagnosed gliosarcoma due to local progression of the tumor. Therefore, the 12-month OS rate was 95.5%. Two tumors demonstrated progression despite treatment within 6 months after surgery, and both recurrences were local. Therefore, the 6-month PFS and local PFS rates were 91%. The maximum length of follow-up was 38.6 months. The median OS was 27.9 months (95% CI lower, 24.8 months; upper, not estimated), the median PFS was 20 months (95% CI lower, 10.3 months; upper, not estimated), and the median local PFS was 22.5 months (95% CI lower, 17.2 months; upper, not estimated).

Among 13 patients with newly diagnosed GBM, the 12-month OS, 6-month PFS, and 6-month local PFS rates after surgical removal of the tumor and PDT were all 100% (Fig. 1). In this subgroup the maximum length of follow-up was 32.0 months. The median OS was 24.8 months (95% CI 18.5–32.0 months), the median PFS was 12.0 months (95% CI 10.3–24.2 months), and the median local PFS was 20.0 months (95% CI 16.2–32.0 months).

In only 1 patient was it possible to evaluate the overall tumor response to treatment. In this case, a newly diagnosed GBM showed complete response 4 months after surgery and PDT.

*Treatment Safety*

Among all 27 patients who received talaporfin sodium the day before surgery, serious adverse events were noted postoperatively in 6 patients (22.2%). These included aphasia (2 cases) and hemiplegia, hemiparesis, unilateral blindness, visual field defect, homonymous hemianopia, postoperative pyrexia, and infection (1 case each). The overall frequency and distribution of postoperative adverse events were within the range of our usual neurosurgical practice in cases of primary malignant parenchymal brain tumors, and their causal relationships with administration of talaporfin sodium and/or intraoperative laser irradiation were very unlikely. None of these adverse events resulted in the death of a patient.

The laboratory test results in all patients were abnormal, most frequently with an increase in γ-glutamyltransferase (59.3%), alanine aminotransferase (48.1%), aspartate aminotransferase (37.0%), blood alkaline phosphatase (25.9%), and blood lactate dehydrogenase (22.2%). In 18 (66.7%) of 27 patients such abnormalities could be considered as side effects after administration of talaporfin sodium. Postoperative adverse events by system organs, particularly abnormal liver function, were relatively frequent but never exceeded Grade 3 toxicity (Table 2). Only 2 patients (7.4%) had skin disorders, which could be con-

**TABLE 1: Characteristics of patients enrolled into study**

| Demographics & Clinical Characteristics | Value* | | |
|---|---|---|---|
| | Initially Enrolled Patients (n = 27) | Study Cohort | |
| | | Total (n = 22) | Newly Diagnosed GBM (n = 13) |
| age in yrs | | | |
| mean ± SD | 47.1 ± 13.5 | 48.1 ± 13.5 | 46.0 ± 14.1 |
| median (range) | 50.0 (24–69) | 50.5 (24–69) | 49.0 (24–69) |
| sex | | | |
| male | 13 (48.1) | 11 (50.0) | 6 (46.2) |
| female | 14 (51.9) | 11 (50.0) | 7 (53.8) |
| histopathological type of tumor† | | | |
| GBM | 13 (48.1) | 13 (59.1) | 13 (100.0) |
| gliosarcoma | 1 (3.7) | 1 (4.5) | 0 (0) |
| anaplastic astrocytoma | 3 (11.1) | 3 (13.6) | 0 (0) |
| anaplastic oligoastrocytoma | 2 (7.4) | 2 (9.1) | 0 (0) |
| anaplastic oligodendroglioma | 2 (7.4) | 2 (9.1) | 0 (0) |
| pilocytic astrocytoma w/ anaplastic features | 1 (3.7) | 1 (4.5) | 0 (0) |
| oligodendroglioma | 2 (7.4) | 0 (0) | 0 (0) |
| central review not performed‡ | 3 (11.1) | 0 (0) | 0 (0) |
| WHO grade† | | | |
| IV | 14 (51.9) | 14 (63.6) | 13 (100.0) |
| III | 8 (29.6) | 8 (36.4) | 0 (0) |
| II | 2 (7.4) | 0 (0) | 0 (0) |
| central review not performed‡ | 3 (11.1) | 0 (0) | 0 (0) |
| tumor status | | | |
| newly diagnosed | 26 (96.3) | 21 (95.5) | 13 (100.0) |
| recurrent | 1 (3.7) | 1 (4.5) | 0 (0) |
| tumor location | | | |
| frontal lobe | 16 (59.3) | 13 (59.1) | 7 (53.8) |
| temporal lobe | 5 (18.5) | 3 (13.6) | 2 (15.4) |
| parietal lobe | 4 (14.8) | 4 (18.2) | 3 (23.1) |
| occipital lobe | 2 (7.4) | 2 (9.1) | 1 (7.7) |
| tumor side | | | |
| rt | 13 (48.1) | 12 (54.5) | 8 (61.5) |
| lt | 14 (51.9) | 10 (45.5) | 5 (38.5) |
| tumor functional grade | | | |
| located in eloquent area | 13 (48.1) | 12 (54.5) | 7 (53.8) |
| adjacent to eloquent area | 6 (22.2) | 4 (18.2) | 2 (15.4) |
| located in noneloquent area | 8 (29.6) | 6 (27.3) | 4 (30.8) |
| PS before treatment§ | | | |
| 0 | 14 (51.9) | 10 (45.5) | 3 (23.1) |
| 1 | 10 (37.0) | 9 (40.9) | 8 (61.5) |
| 2 | 0 (0) | 0 (0) | 0 (0) |
| 3 | 3 (11.1) | 3 (13.6) | 2 (15.4) |
| extent of tumor resection | | | |
| total | 9 (33.3) | 8 (36.4) | 5 (38.5) |
| subtotal (>90% of lesion vol) | 13 (48.1) | 11 (50.0) | 8 (61.5) |
| partial | 5 (18.5) | 3 (13.6) | 0 (0) |

* Unless otherwise stated, values represent cases (%).
† According to central review based on WHO criteria.
‡ These patients did not receive laser irradiation during surgery due to results of the intraoperative histopathological investigation of the resected tissue on the frozen sections and exclusion of the diagnosis of primary malignant parenchymal brain tumor.
§ According to the Eastern Cooperative Oncology Group Performance Status Scale.

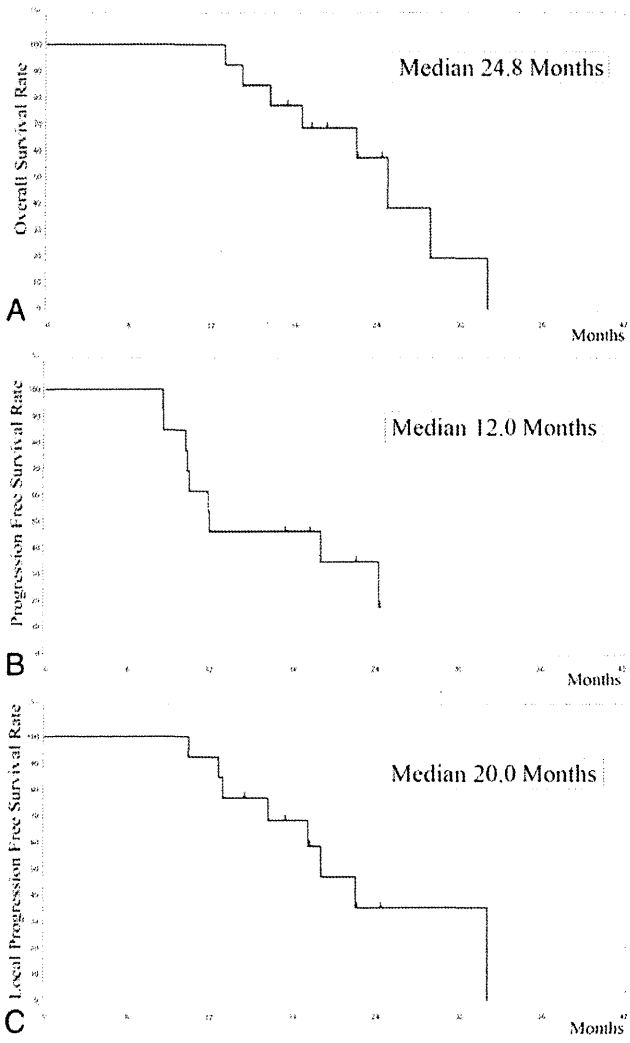


FIG. 1. Kaplan-Meier curves for OS **(A)**, PFS **(B)**, and local PFS **(C)** in the subgroup of patients with newly diagnosed GBM included in the study cohort. Censored observations are marked.

sidered as side effects after administration of talaporfin sodium. It included rash (2 cases), blister (1 case), and erythema (1 case).

Photosensitivity test results were relatively mild and most patients had a score of 1 (barely perceptible erythema) or 2 (distinct erythema); no patient had a score of 3 (marked erythema or edema). These reactions completely disappeared within 4, 8, and 15 days after administration of talaporfin sodium in 55.6%, 77.8%, and 100% of patients, respectively (Table 3).

## Discussion

Management of primary malignant parenchymal brain tumors represents a significant challenge. According to the latest edition of the Japan Brain Tumor Registry, 1-, 2-, and 3-year survival rates of patients with high-grade gliomas constitute 64%, 37%, and 28%, respectively.[5] The poor survival rates are mainly due to an inability to perform complete removal of the neoplasm due to its infiltrative growth into functionally important neuronal structures, as well as the limited effectiveness of the postoperative radiotherapy and chemotherapy. Therefore, finding additional effective and safe treatment options in such cases is required.

As a highly selective treatment with minimal injury to the adjacent normal structures, PDT has demonstrated promising potential for management of the various cancers and nonneoplastic disorders, such as age-related macular degeneration, local infection, dermatological diseases, arteriosclerosis, and rheumatoid arthritis.[7] However, despite a large amount of basic and clinical research conducted during several decades and directed on testing of the various photosensitizers, light sources, irradiation types, and treatment regimens, PDT still was not approved to be used as a standard treatment for malignant brain tumors.[2,10] During the last decade there was considerable interest in the use of 5-aminolevulinic acid (5-ALA) in the surgical management of gliomas. Nevertheless, while its application for photodynamic diagnosis and fluorescence-guided resection was associated with a significant impact on effectiveness of tissue sampling, tumor resection rates, and clinical outcomes,[4,17] the attempts to use this photosensitizer for PDT were not so impressive.[2] These unimpressive results might be particularly caused by insufficient incorporation of the drug in the neoplastic cells, especially in necrotic regions and at the periphery of the neoplasm.[2]

In the present study PDT was based on administration of the relatively novel second-generation photosensitizer talaporfin sodium. This water-soluble compound is derived from plant chlorophyll. In the living body it binds to albumin and does not pass the blood-brain barrier. In neoplastic cells it is primarily distributed in the lysosomes.[14] Compared with conventional photosensitizers, talaporfin sodium is activated by light with longer wavelengths; therefore, its light absorption is not affected by hemoglobin and penetrates deeper.[13] Additionally, talaporfin sodium more selectively accumulates in glioma tissue, is rapidly eliminated from the normal tissues, and is less likely to cause adverse reactions.[14] It was demonstrated that PDT based on administration of talaporfin sodium with subsequent irradiation using a 664-nm laser led to necrosis and apoptosis of cultured human glioblastoma cells[13] and experimental tumors[14] in a dose- and time-dependent fashion. The adverse effects on the peritumoral brain were limited to mild temporary edema, and no damage to neurons or the myelin sheath was observed.[14] A pilot clinical study on 14 adult patients with unresectable malignant gliomas showed a median PFS of 23 months in newly diagnosed neoplasms.[1] In concordance, in our present prospective investigation, which included 21 patients with newly diagnosed high-grade gliomas treated according to strict research protocol, the median local PFS constituted 22.5 months.

The most impressive results of our study were obtained in patients with a newly diagnosed GBM. In this subgroup, the 12-month OS and 6-month PFS rates were 100%, and the median OS and median PFS were 24.8 and 12.0 months, respectively. These rates compare favorably

**TABLE 2: Frequency of adverse events and side effects by grade***

| System Organ Class† | No. of Patients (%) | | | | | |
|---|---|---|---|---|---|---|
| | Grade 1 | Grade 2 | Grade 3 | Grade 4 | Grade 5 | Total (n = 27) |
| adverse events | | | | | | |
| investigations | 3 (11.1) | 12 (44.4) | 10 (37.0) | 2 (7.4) | 0 (0.0) | 27 (100.0) |
| gastrointestinal disorders | 5 (18.5) | 16 (59.3) | 0 (0.0) | 0 (0.0) | 0 (0.0) | 21 (77.8) |
| general disorders & administration site conditions | 15 (55.6) | 6 (22.2) | 0 (0.0) | 0 (0.0) | 0 (0.0) | 21 (77.8) |
| nervous system disorders | 1 (3.7) | 17 (63.0) | 2 (7.4) | 0 (0.0) | 0 (0.0) | 20 (74.1) |
| skin & subcutaneous tissue disorders | 10 (37.0) | 8 (29.6) | 0 (0.0) | 0 (0.0) | 0 (0.0) | 18 (66.7) |
| injury, poisoning, & procedural complications | 9 (33.3) | 6 (22.2) | 0 (0.0) | 0 (0.0) | 0 (0.0) | 15 (55.6) |
| eye disorders | 7 (25.9) | 1 (3.7) | 1 (3.7) | 0 (0.0) | 0 (0.0) | 9 (33.3) |
| infections & infestations | 1 (3.7) | 3 (11.1) | 2 (7.4) | 0 (0.0) | 0 (0.0) | 6 (22.2) |
| renal & urinary disorders | 3 (11.1) | 2 (7.4) | 0 (0.0) | 0 (0.0) | 0 (0.0) | 5 (18.5) |
| psychiatric disorders | 4 (14.8) | 0 (0.0) | 0 (0.0) | 0 (0.0) | 0 (0.0) | 4 (14.8) |
| respiratory, thoracic, & mediastinal disorders | 4 (14.8) | 0 (0.0) | 0 (0.0) | 0 (0.0) | 0 (0.0) | 4 (14.8) |
| vascular disorders | 0 (0.0) | 0 (0.0) | 4 (14.8) | 0 (0.0) | 0 (0.0) | 4 (14.8) |
| musculoskeletal & connective tissue disorders | 1 (3.7) | 2 (7.4) | 0 (0.0) | 0 (0.0) | 0 (0.0) | 3 (11.1) |
| blood & lymphatic system disorders | 1 (3.7) | 1 (3.7) | 0 (0.0) | 0 (0.0) | 0 (0.0) | 2 (7.4) |
| metabolism & nutrition disorders | 0 (0.0) | 0 (0.0) | 2 (7.4) | 0 (0.0) | 0 (0.0) | 2 (7.4) |
| cardiac disorders | 1 (3.7) | 0 (0.0) | 0 (0.0) | 0 (0.0) | 0 (0.0) | 1 (3.7) |
| ear & labyrinth disorders | 1 (3.7) | 0 (0.0) | 0 (0.0) | 0 (0.0) | 0 (0.0) | 1 (3.7) |
| side effects | | | | | | |
| investigations | 7 (25.9) | 6 (22.2) | 5 (18.5) | 0 (0.0) | 0 (0.0) | 18 (66.7) |
| skin & subcutaneous tissue disorders | 1 (3.7) | 1 (3.7) | 0 (0.0) | 0 (0.0) | 0 (0.0) | 2 (7.4) |

* According to the Cancer Therapy Evaluation Program.[3]
† According to the Medical Dictionary for Regulatory Activities version 14.1 (http://www.meddra.org).

with contemporary results obtained in such tumors with standard treatment. In a global Phase III randomized controlled study on radiotherapy with concomitant and adjuvant temozolomide for GBM, Stupp et al.[18] demonstrated a 12-month OS rate of 61%, a 6-month PFS rate of 54%, a median OS of 14.6 months, and a median PFS of 6.9 months. In the series by Stummer et al.[17] on fluorescence-guided resection of malignant gliomas with the use of 5-ALA, the 6-month PFS rate was 41% and the median PFS period was 5.1 months. Moreover, in our patients with a newly diagnosed GBM, the median local PFS was nearly two times longer than the median PFS (20.0 vs 12.0 months). It can therefore be speculated that prolonged survival was caused by improved local tumor growth control due to intraoperative PDT. It should be emphasized that in the present series all patients with newly diagnosed GBM underwent either total or subtotal resection. Aggressive removal of the tumor may be an important prerequisite for clinical effectiveness of intraoperative PDT, since the penetration depth of a laser is approximately 2.5–5 mm; therefore, the corresponding effective distance for irradiation is limited to 0.75–1.5 cm.[1,2] The limitations of the efficacy of PDT in bulky target tissues and recurrent tumors have been demonstrated.[1] It is also possible that metabolically active infiltrating tumor cells in the periphery of the GBM may be more sensitive to PDT because of incorporation of a greater amount of photosensitizer. It was reported that the tissue concentration of a photosensitizer directly correlates with the grade of malignancy of the neoplasm.[2]

In the present study PDT showed a high level of safe-

**TABLE 3: Skin photosensitivity test results in 27 patients***

| No. of Days† | No. of Patients (%) | Cumulative No. of Patients (%) |
|---|---|---|
| 3 | 4 (14.8) | 4 (14.8) |
| 4 | 11 (40.7) | 15 (55.6) |
| 8 | 6 (22.2) | 21 (77.8) |
| 10 | 1 (3.7) | 22 (81.5) |
| 13 | 2 (7.4) | 24 (88.9) |
| 14 | 1 (3.7) | 25 (92.6) |
| 15 | 2 (7.4) | 27 (100) |

* For the skin photosensitivity test, between 11 a.m. and 2 p.m., the back of the individual's hand was exposed to direct sunlight for 5 minutes, and the occurrence of any photosensitivity reaction, such as erythema, was assessed. In cases in which photosensitivity reactions were detected, the subject was kept shielded from light until the reaction disappeared, and the skin photosensitivity test was subsequently repeated.
† From administration of talaporfin sodium to disappearance of reaction.

ty. While laboratory investigations have frequently revealed abnormalities likely attributable to the administration of talaporfin sodium, only 2 patients (7.4%) had definite symptoms on the skin, which did not exceed Grade 2 toxicity. In no case did we encounter brain edema or cerebral infarction, which may complicate PDT.[1,2] Therefore, the risk of clinically significant side effects caused by the administration of talaporfin sodium and intraoperative irradiation of the residual tumor and peritumoral brain with a 664-nm laser 22–27 hours thereafter may be considered low. Moreover, according to photosensitivity test results, any reactions completely disappeared in all patients within 15 days after administration of the drug.

The main limitations of the present study are related to its design. A nonrandomized noncontrolled prospective investigation was performed in just 2 neurosurgical centers with well-established neurooncology programs and enrolled a limited number of highly selected cases with rather heterogeneous histopathological diagnoses of malignant parenchymal brain tumors. It is evident that to prove clinical efficacy of the intraoperative PDT with talaporfin sodium and a semiconductor laser, further carefully designed Phase III studies should be performed in a sufficiently large number of patients with possible initial stratification according to tumor resection rate. Testing of the proposed treatment method is also planned in cases of low-grade gliomas and in incompletely resected benign extraaxial neoplasms, such as pituitary adenomas and meningiomas. Since appropriate use of equipment for PDT requires specific skills, the dedicated training program for neurosurgeons is currently under organization. Finally, advanced experimental investigations directed at further understanding the basic mechanisms of the therapeutic effectiveness of intraoperative PDT are also required, and additional studies to search for the most optimal treatment regimens should be continued as well.

## Conclusions

The results of the present study demonstrate that novel PDT based on administration of talaporfin sodium and subsequent irradiation with a 664-nm semiconductor laser may provide an additional benefit to the combined management of primary malignant parenchymal brain tumors through possible improvement of their local growth control, which, in turn, may lead to prolongation of the patient's survival. The therapy seems sufficiently safe with a minimal risk of serious side effects. Therefore, application of the intraoperative PDT along with aggressive resection, radiotherapy, and chemotherapy may be of clinical significance, particularly in patients with newly diagnosed GBM.

### Disclosure

This study was supported by grants of an open-label study of photodynamic therapy with ME2906 and PNL6405CNS in patients with malignant brain tumors by Center for Clinical Trials, Japan Medical Association, Funding Program for World-Leading Innovative R&D on Science and Technology (FIRST Program) by the Japan Society for the Promotion of Science (JSPS), and Strategic international standardization acceleration action plan by METI (Ministry of Economy, Trade and Industry).

Author contributions to the study and manuscript preparation include the following. Conception and design: Muragaki, Akimoto, Iseki, Maebayashi, Matsumura, Kuroiwa, Nakazato, Kayama. Acquisition of data: Muragaki, Akimoto, Ikuta, Nitta, Saito, Kaneko. Analysis and interpretation of data: Muragaki, Akimoto, Ikuta, Karasawa. Drafting the article: Muragaki. Critically revising the article: all authors. Reviewed submitted version of manuscript: all authors. Approved the final version of the manuscript on behalf of all authors: Muragaki. Statistical analysis: Muragaki, Ikuta. Administrative/technical/material support: Maruyama, Iseki, Nitta, Maebayashi, Saito, Okada, Kaneko, Matsumura, Kuroiwa, Karasawa, Nakazato, Kayama. Study supervision: Muragaki, Iseki, Maebayashi, Okada, Matsumura, Kuroiwa, Nakazato, Kayama.

### Acknowledgments

The authors thank all of the patients who participated in this study and the investigators from both study sites. Special thanks are devoted to Drs. Masahiko Tanaka, Norio Mitsuhashi, and Mikhail Chernov, and Mr. Takashi Sakayori (Tokyo Women's Medical University) for valuable help with clinical work and data analysis.

### References

1. Akimoto J, Haraoka J, Aizawa K: Preliminary clinical report on safety and efficacy of photodynamic therapy using talaporfin sodium for malignant gliomas. **Photodiagn Photodyn Ther 9:**91–99, 2012
2. Bechet D, Mordon SR, Guillemin F, Barberi-Heyob MA: Photodynamic therapy of malignant brain tumours: a complementary approach to conventional therapies. **Cancer Treat Rev** [epub ahead of print], 2012
3. Cancer Therapy Evaluation Program: Common Terminology Criteria for Adverse Events v3.0 (CTCAE). **ctep.cancer.gov.** (http://ctep.cancer.gov/protocolDevelopment/electronic_applications/docs/ctcaev3.pdf) [Accessed July 22, 2013]
4. Colditz MJ, Jeffree RL: Aminolevulinic acid (ALA)-protoporphyrin IX fluorescence guided tumour resection. Part 1: Clinical, radiological and pathological studies. **J Clin Neurosci 19:**1471–1474, 2012
5. Committee of Brain Tumor Registry of Japan: Report of brain tumor registry of Japan (1984–2000), 12 edition. **Neurol Med Chir (Tokyo) 49 (Suppl):**1–101, 2009
6. Curran WJ Jr, Scott CB, Horton J, Nelson JS, Weinstein AS, Fischbach AJ, et al: Recursive partitioning analysis of prognostic factors in three Radiation Therapy Oncology Group malignant glioma trials. **J Natl Cancer Inst 85:**704–710, 1993
7. Dougherty TJ, Gomer CJ, Henderson BW, Jori G, Kessel D, Korbelik M, et al: Photodynamic therapy. **J Natl Cancer Inst 90:**889–905, 1998
8. Juzeniene A, Peng Q, Moan J: Milestones in the development of photodynamic therapy and fluorescence diagnosis. **Photochem Photobiol Sci 6:**1234–1245, 2007
9. Konishi Y, Muragaki Y, Iseki H, Mitsuhashi N, Okada Y: Patterns of intracranial glioblastoma recurrence after aggressive surgical resection and adjuvant management: retrospective analysis of 43 cases. **Neurol Med Chir (Tokyo) 52:**577–586, 2012
10. Kostron H: Photodynamic diagnosis and therapy and the brain. **Methods Mol Biol 635:**261–280, 2010
11. Louis DN, Ohgaki H, Wiestler OD, Cavenee WK (eds): **WHO Classification of Tumours of the Central Nervous System, ed 4.** Lyon: IARC Press, 2007
12. Matsumura H, Akimoto J, Haraoka J, Aizawa K: Uptake and retention of the photosensitizer mono-L-asparthyl chlorine e6 in experimental malignant glioma. **Lasers Med Sci 23:**237–245, 2008

13. Miki Y, Akimoto J, Yokoyama S, Homma T, Tsutsumi M, Haraoka J, et al: Photodynamic therapy in combination with talaporfin sodium induces mitochondrial apoptotic cell death accompanied with necrosis in glioma cells. **Biol Pharm Bull 36:**215–221, 2013
14. Namatame H, Akimoto J, Matsumura H, Haraoka J, Aizawa K: Photodynamic therapy of C6-implanted glioma cells in the rat brain employing second-generation photosensitizer talaporfin sodium. **Photodiagn Photodyn Ther 5:**198–209, 2008
15. Palumbo G: Photodynamic therapy and cancer: a brief sightseeing tour. **Expert Opin Drug Deliv 4:**131–148, 2007
16. Petrecca K, Guiot MC, Panet-Raymond V, Souhami L: Failure pattern following complete resection plus radiotherapy and temozolomide is at the resection margin in patients with glioblastoma. **J Neurooncol 111:**19–23, 2013
17. Stummer W, Pichlmeier U, Meinel T, Wiestler OD, Zanella F, Reulen HJ: Fluorescence-guided surgery with 5-aminolevulinic acid for resection of malignant glioma: a randomised controlled multicentre phase III trial. **Lancet Oncol 7:**392–401, 2006
18. Stupp R, Mason WP, van den Bent MJ, Weller M, Fisher B, Taphoorn MJ, et al: Radiotherapy plus concomitant and adjuvant temozolomide for glioblastoma. **N Engl J Med 352:**987–996, 2005

Manuscript submitted February 28, 2013.
Accepted July 16, 2013.
Please include this information when citing this paper: published online August 16, 2013; DOI: 10.3171/2013.7.JNS13415.
*Address correspondence to*: Yoshihiro Muragaki, M.D., Ph.D., Faculty of Advanced Techno-Surgery, Institute of Advanced Biomedical Engineering and Science, Tokyo Women's Medical University, 8-1 Kawada-cho, Shinjuku-ku, Tokyo 162-8666, Japan. email: ymuragaki@abmes.twmu.ac.jp.

Neurol Med Chir (Tokyo) 53, 447 ~ 454, 2013

# The 71st Annual Meeting Special Topics — Part III: Treatment Strategy of Low Grade Glioma

## *Updated Therapeutic Strategy for Adult Low-Grade Glioma Stratified by Resection and Tumor Subtype*

Masayuki NITTA,[1,2] Yoshihiro MURAGAKI,[1,2] Takashi MARUYAMA,[1,2] Hiroshi ISEKI,[1,2] Soko IKUTA,[2] Yoshiyuki KONISHI,[2] Taichi SAITO,[1] Manabu TAMURA,[2] Michael CHERNOV,[2] Atsushi WATANABE,[1,2] Saori OKAMOTO,[1,2] Katsuya MAEBAYASHI,[3] Norio MITSUHASHI,[3] and Yoshikazu OKADA[1]

[1]*Department of Neurosurgery,* [2]*Faculty of Advanced Techno-Surgery, and* [3]*Department of Radiation Oncology, Graduate School of Medicine, Tokyo Women's Medical University, Tokyo*

### Abstract

**The importance of surgical resection for patients with supratentorial low-grade glioma (LGG) remains controversial. This retrospective study of patients (n = 153) treated between 2000 to 2010 at a single institution assessed whether increasing the extent of resection (EOR) was associated with improved progression-free survival (PFS) and overall survival (OS). Histological subtypes of World Health Organization grade II tumors were as follows: diffuse astrocytoma in 49 patients (32.0%), oligoastrocytoma in 45 patients (29.4%), and oligodendroglioma in 59 patients (38.6%). Median pre- and postoperative tumor volumes and median EOR were 29.0 $cm^3$ (range 0.7–162 $cm^3$) and 1.7 $cm^3$ (range 0–135.7 $cm^3$) and 95%, respectively. Five- and 10-year OS for all LGG patients were 95.1% and 85.4%, respectively. Eight-year OS for diffuse astrocytoma, oligoastrocytoma, and oligodendroglioma were 70.7%, 91.2%, and 98.3%, respectively. Five-year PFS for diffuse astrocytoma, oligoastrocytoma, and oligodendroglioma were 42.6%, 71.3%, and 62.7%, respectively. Patients were divided into two groups by EOR ≥ 90% and < 90%, and OS and PFS were analyzed. Both OS and PFS were significantly longer in patients with ≥ 90% EOR. Increased EOR resulted in better PFS for diffuse astrocytoma but not for oligodendroglioma. Multivariate analysis identified age and EOR as parameters significantly associated with OS. The only parameter associated with PFS was EOR. Based on these findings, we established updated therapeutic strategies for LGG. If surgery resulted in EOR < 90%, patients with astrocytoma will require second-look surgery, whereas patients with oligodendroglioma or oligoastrocytoma, which are sensitive to chemotherapy, will be treated with chemotherapy.**

Key words: low-grade glioma, treatment strategy, extent of resection, survival, residual tumor volume

## Introduction

Low-grade glioma (LGG) has a more favorable prognosis than its malignant counterparts. The median survival for patients with LGGs is 5–10 years.[5,11,18] The slow growth of LGG requires extensive follow up, and therefore there are few evidence-based standards for guiding the medical and surgical treatment of patients with LGGs. Despite long-term survival, patients with LGG eventually die of either progression of the low-grade tumor or malignant transformation.[9] Compared with high-grade glioma, little is known about the factors that may predict survival of patients with LGGs. Historically, age, size of the tumor, tumor location, tumor subtype, and neurological deficit have been used as preoperative prog-

Received March 3, 2013; Accepted May 9, 2013

nostic factors for LGGs,[1,19] and the importance of surgical resection has not been emphasized.[9] However, emerging evidence suggests a strong correlation between extent of resection (EOR) and patient survival over 5 years.[12,21,23] The present retrospective study assessed the influence of EOR on outcome in patients with LGGs, and attempted to establish therapeutic strategies for LGG based on EOR and tumor subtype.

## Methods

We conducted a retrospective review with long-term follow up of 153 patients (age ≥15 years, 84 males and 69 females) with supratentorial infiltrative LGG treated with surgical resection or biopsy at Tokyo Women's Medical University (TWMU) between January 2000 and August 2010. Patients were excluded if they had undergone prior resection of the tumor, with the exception of previous biopsy procedures performed as part of a diagnostic workup leading to eventual surgical removal in TWMU. Patients with neurofibromatosis type 1, pleomorphic xanthoastrocytoma, or infratentorial lesions were also excluded. Tumor grading and pathological diagnosis were performed based on World Health Organization (WHO) guidelines.[10] Clinical data were collected from patient records and telephone interviews. Two outcome measures were assessed: overall survival (OS) and progression-free survival (PFS). OS was defined as the time between initial surgery and death, whereas PFS was defined as the time between initial surgery and demonstration of unequivocal increase in tumor size on follow-up imaging, malignant progression, and/or death. Patients with no known progression/malignant progression were censored as of their last visit/scan date.

Tumor volumes as determined from axial $T_2$-weighted magnetic resonance (MR) imaging were calculated by importing Digital Imaging and Communications in Medicine (DICOM) images from the MR scanner to Leksell GammaPlan® software (Elekta AB, Stockholm, Sweden). EOR was calculated as: (preoperative tumor volume − postoperative tumor volume)/preoperative tumor volume.

OS and PFS were estimated using Kaplan-Meier method. A log-rank test was used to evaluate the importance of prognostic factors that might affect survival. Data analysis was performed using the JMP® statistical software (SAS Institute, Cary, North Carolina, USA). Univariate analyses for OS and PFS were performed using Cox proportional-hazards modeling. Variables that were statistically significant or showed borderline significance on univariate analysis were further analyzed with multivariate analysis using Cox proportional-hazards modeling. Hazard ratios (HRs) and 95% confidence intervals (CIs) are reported with the two-tailed probability values. The reported probability values in the Cox model are based on the World test, and values of $<0.05$ were considered significant.

## Results

Patient demographics and tumor characteristics are

**Table 1 Clinical and tumor characteristics of patients with low-grade glioma (N = 153)**

| Characteristics | |
|---|---|
| Sex | |
| male | 84 (54.9%) |
| female | 69 (45.1%) |
| Age | |
| <50 yrs | 116 (75.8%) |
| ≥50 yrs | 37 (24.2%) |
| median | 37 yrs |
| range | 15–76 yrs |
| KPS at diagnosis | |
| 100 | 121 (79.1%) |
| 90 | 27 (17.6%) |
| <90 | 5 (3.3%) |
| median | 100 |
| range | 70–100 |
| Tumor subtype | |
| diffuse astrocytoma | 49 (32.0%) |
| oligoastrocytoma | 45 (29.4%) |
| oligodendroglioma | 59 (38.6%) |
| Postoperative radiation therapy | |
| yes | 48 (31.4%) |
| no | 105 (68.6%) |
| Postoperative chemotherapy | |
| yes | 35 (22.9%) |
| no | 118 (77.1%) |
| Preoperative maximum tumor diameter | |
| median | 4.75 cm |
| range | 1–10.5 cm |
| Preoperative tumor volume | |
| median | 29.0 $cm^3$ |
| range | 0.7–162 $cm^3$ |
| mean | 38.4 $cm^3$ |
| Postoperative tumor volume | |
| median | 1.7 $cm^3$ |
| range | 0–135.7 $cm^3$ |
| mean | 9.3 $cm^3$ |
| Extent of resection | |
| <90% | 59 (38.6%) |
| ≥90% | 94 (61.4%) |
| median | 95% |
| 95% CI | 77.0–85.7% |
| mean | 81.4% |

KPS: Karnofsky performance status.

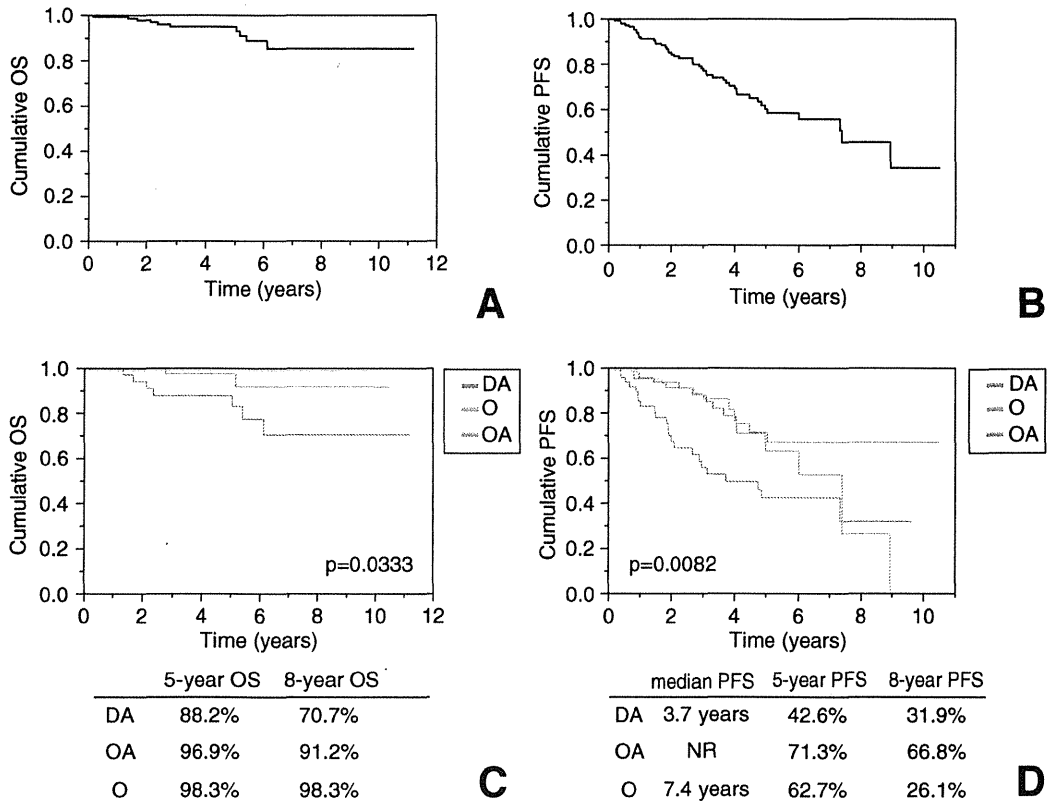


| | 5-year OS | 8-year OS |
|---|---|---|
| DA | 88.2% | 70.7% |
| OA | 96.9% | 91.2% |
| O | 98.3% | 98.3% |

C

| | median PFS | 5-year PFS | 8-year PFS |
|---|---|---|---|
| DA | 3.7 years | 42.6% | 31.9% |
| OA | NR | 71.3% | 66.8% |
| O | 7.4 years | 62.7% | 26.1% |

D

**Fig. 1 A, B: Kaplan-Meier plots showing overall survival (OS) (A) and progression-free survival (PFS) (B) for all patients with low-grade glioma. C, D: Kaplan-Meier plots showing poorer OS for diffuse astrocytoma than oligodendroglial subtypes (C), but no statistical difference in PFS between tumor subtypes (D). DA: diffuse astrocytoma, NR: not reached, O: oligodendroglioma, OA: oligoastrocytoma.**

described in Table 1. Median age was 37.0 years (range 15–76 years). Median time between symptom onset and time of surgical resection was 6.4 months (range 21 days to 18.7 years). The histological subtypes of WHO grade II tumors were as follows: diffuse astrocytoma in 49 patients (32.0%), oligoastrocytoma in 45 patients (29.4%), and oligodendroglioma in 59 patients (38.6%). Median Ki-67 proliferation index was 4.2% (range 0.3–21.0%). Radiation was administered to 48 patients (31.4%) and ACNU-based chemotherapy was given to 35 patients (22.9%). Median time to progression was 2.94 years, and median time to malignant progression was 2.24 years.

Five-, 8-, and 10-year OS for all patients analyzed were 95.1%, 85.4%, and 85.4%, respectively (Fig. 1A). Median PFS, 5-, 8-, and 10-year PFS were 7.3 years, 60.2%, 45.7%, and 34.3%, respectively (Fig. 1B). Eight-year OS for diffuse astrocytoma, oligoastrocytoma, and oligodendroglioma were 70.7%, 91.2%, and 98.3%, respectively (Fig. 1C). Five-year PFS for diffuse astrocytoma, oligoastrocytoma, and oligodendroglioma were 42.6%, 71.3%, and 62.7%, respectively (Fig. 1D). Diffuse astrocytoma showed significantly poorer prognosis compared to oligoastrocytoma and oligodendroglioma ($p = 0.033$).

Median and mean volumes of the preoperative tumor were 29.0 $cm^3$ (range 0.7–162 $cm^3$) and 38.4 $cm^3$, respectively. Median and mean volumes of the postoperative tumor were 1.7 $cm^3$ (range 0–135.7 $cm^3$) and 9.3 $cm^3$, respectively. One perioperative death due to pulmonary embolization was encountered. A total of 146 patients (95.4%) underwent surgical resection and intraoperative MR imaging was used in 140 (95.9%) patients. Seven patients (4.6%) underwent biopsy. Overall, median and mean EOR were 95.0% and 81.4% (95% CI 77.0–85.7%), respectively. EOR of 90% or more was achieved in 94 patients (61.4%) and EOR of less than 90% in 59 patients (38.6%).

Patients were divided into two groups by EOR $\geq 90\%$ and $< 90\%$, and OS and PFS were analyzed. Both OS and PFS were significantly longer in patients with $\geq 90\%$ EOR (Fig. 2A, B). To see if less residual tumor volume is important for outcome, patients were divided by residual tumor volume $< 5$

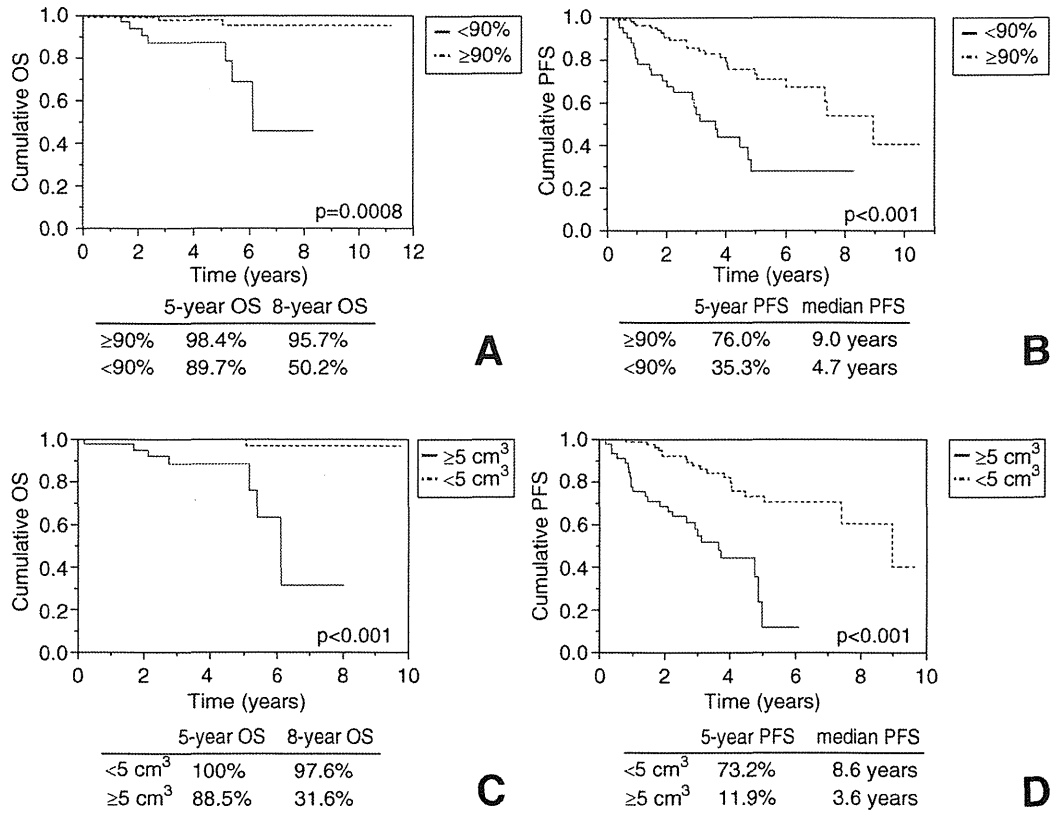


**Fig. 2 Importance of extent of resection (EOR) for patient prognosis. A, B: Kaplan-Meier plots showing overall survival (OS) (A) and progression-free survival (PFS) (B) in patients with ≥90% and <90% EOR. C, D: Kaplan-Meier plots showing OS (C) and PFS (D) in patients with <5 cm³ and ≥5 cm³ residual tumor volume. Both EOR and residual tumor volume are strongly correlated with patient outcome.**

$cm^3$ and ≥5 $cm^3$. As expected, patients with <5 $cm^3$ of residual tumor volume showed better OS and PFS (Fig. 2C, D). These results strongly suggested that EOR ≥90% and decreased residual tumor volume are associated with better outcomes (Fig. 2).

We then addressed how EOR affects patient prognosis for each histological subtype. Because the number of patients was not adequate to analyze OS, the correlations between EOR, residual tumor volume, and PFS were investigated. Interestingly, patients with diffuse astrocytoma and oligoastrocytoma showed a significant difference in PFS between the group with ≥90% EOR and <90% EOR (Fig. 3A, B). Conversely, in patients with oligodendroglioma, EOR did not correlate with PFS (Fig. 3C). To confirm these results, the correlation between the volume of the residual tumor and patient prognosis was investigated. As expected, patients with astrocytoma and oligoastrocytoma, if residual tumor volume was <5 $cm^3$, showed significantly longer PFS, whereas residual tumor volume did not affect PFS in patients with oligodendroglioma (Fig. 3D–F).

Univariate analysis on Cox proportional hazards model selected age (HR 5.43, 95% CI 1.55–21.30; p = 0.009), EOR (HR 8.25, 95% CI 2.26–38.73; p = 0.001), and tumor subtype (HR, 4.98, 95% CI 1.37–23.27; p = 0.0143) for OS (Table 2). Parameters selected for PFS were EOR (HR 3.40, 95% CI 1.88–6.12; p < 0.0001) and tumor subtype (HR 2.09, 95% CI 1.16–3.72; p = 0.014) (Table 2). Neither tumor diameter nor MIB-1 index affected the prognosis (Table 2).

Multivariate modeling was performed for each outcome measure using the following parameters: age, maximum tumor diameter, EOR, tumor subtype, and MIB-1 index. The parameters identified as significant for OS were age (HR 4.08, 95% CI 1.08–16.86; p = 0.038) and EOR (HR 4.75, 95% CI 1.07–26.48; p = 0.039) (Table 2). The only parameter selected for PFS was EOR (HR 2.69, 95% CI 1.43–5.04; p = 0.002) (Table 2). Thus, EOR showed the strongest correlation with patient survival (Table 2).

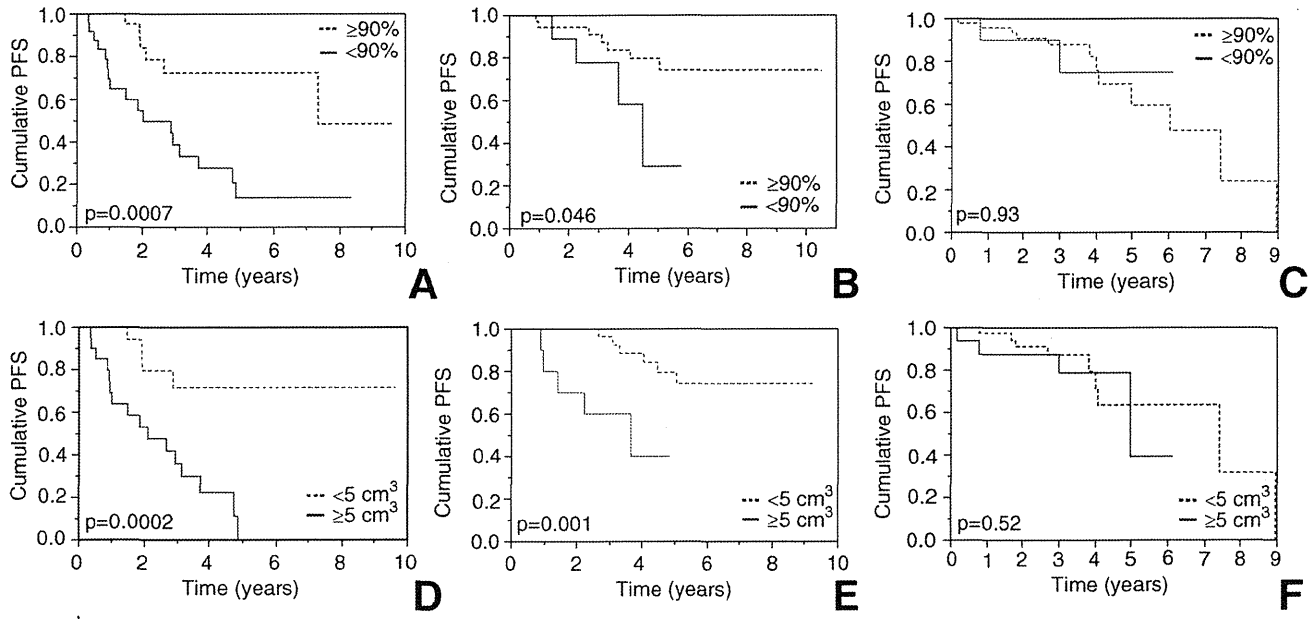


**Fig. 3 Different effects of extent of resection (EOR) on patient progression-free survival (PFS) between tumor subtypes. A–C: Kaplan-Meier plots showing that ≥ 90% EOR resulted in better PFS in patients with diffuse astrocytoma (A) and oligoastrocytoma (B) but not in oligodendroglioma (C). D–F: Patients with < 5 cm³ of residual tumor volume showed longer PFS in patients with diffuse astrocytoma (D) and oligoastrocytoma (E) but not in oligodendroglioma (F).**

**Table 2 Univariate and multivariate analysis**

For overall survival

| Factor | Univariate | | | Multivariate | | |
|---|---|---|---|---|---|---|
| | HR | 95% CI | p Value | HR | 95% CI | p Value |
| Age: ≥50 yrs vs. <50 yrs | 5.43 | 1.55–21.30 | **0.0089*** | **4.08** | 1.08–16.86 | **0.0375*** |
| Tumor diameter: ≥5 cm vs. <5 cm | 1.2 | 0.43–5.97 | 0.5087 | 0.95 | 0.23–4.08 | 0.9468 |
| Extent of resection: <90% vs. ≥90% | 8.25 | 2.26–38.73 | **0.0014*** | **4.75** | 1.07–26.48 | **0.0391*** |
| Tumor subtype: DA vs. O/OA | 4.98 | 1.37–23.27 | **0.0143*** | 2.64 | 0.62–13.79 | 0.1918 |
| MIB-1 index: ≥5% vs. <5% | 1.53 | 0.42–5.54 | 0.5024 | 1.69 | 0.45–6.38 | 0.4203 |

For progression-free survival

| Factor | Univariate | | | Multivariate | | |
|---|---|---|---|---|---|---|
| | HR | 95% CI | p Value | HR | 95% CI | p Value |
| Age: ≥50 yrs vs. <50 yrs | 1.58 | 0.80–2.93 | 0.1757 | 1.36 | 0.68–2.56 | 0.3665 |
| Tumor diameter: ≥5 cm vs. <5 cm | 1.59 | 0.89–2.89 | 0.1122 | 1.42 | 0.78–2.62 | 0.2503 |
| Extent of resection: <90% vs. ≥90% | 3.4 | 1.88–6.12 | **<0.0001*** | **2.69** | 1.43–5.04 | **0.0022*** |
| Tumor subtype: DA vs. O/OA | 2.09 | 1.16–3.72 | **0.0140*** | 1.7 | 0.92–3.12 | 0.0888 |
| MIB-1 index: ≥5% vs. <5% | 1.94 | 0.51–1.69 | 0.4328 | 0.94 | 0.51–1.70 | 0.8589 |

*p < 0.05. CI: confidence interval, DA: diffuse astrocytoma, HR: hazards ratio, O: oligodendroglioma, OA: oligoastrocytoma.

## Discussion

The management of LGG remains controversial. Due to diffuse infiltration, LGG is usually not considered surgically curable,[20] and biopsy without resection is theoretically acceptable until better evi-